

## Global Pattern of the Magnetic Field Vector Above Neutral Lines from 1974 to 1982: Pic-du-Midi Observations of Prominences

V. Bommier

*Laboratoire 'Atomes et Molécules en Astrophysique', CNRS URA 812-DAMAp, Observatoire de Paris, Section de Meudon, F-92195 Meudon, France E-mail: Veronique.Bommier@obspm.fr*

J.L. Leroy<sup>1</sup>

*I.A.C.-T.H.É.M.I.S., E-38200 La Laguna, Tenerife, Canary Islands, Spain E-mail: leroy@themis.iac.es*

**Abstract.** The magnetic field vectors derived from the Hanle effect measured in prominences during the ascending phase and maximum of Cycle 21 have been plotted on the corresponding synoptic maps of Meudon Observatory (e.g., Figure 2). Most of these measurements have been performed in a single line, He I D3. Our previous analysis of 2-line measurements have already proven that prominence magnetic fields have Inverse polarity (Bommier et al. 1994) and remain close to the horizontal plane (Bommier et al. 1986, 1994). We also found earlier that the field component along the filament axis shows a remarkable large scale pattern, especially at high latitudes (Leroy et al. 1983). Given the geometry of horizontal Inverse field, we reinvestigate this large scale organization through our complete set of observations (296 prominences). These new maps fully confirm and extend to medium latitudes the law of reversal of the axial field from one prominence band to the adjacent ones (see Figure 2). This behavior, together with the Inverse polarity pattern, gives a picture consistent with a North-South global field distorted by the differential rotation (see Figure 3).

### 1. Data Sample

From our full sample of 3297 measurements achieved in 379 quiescent prominences observed at the Pic-du-Midi during the ascending phase of Cycle 21 (1974–1982), we have discarded those prominences for which the identification of the neutral line is doubtful (64 prominences). We have discarded those measurements that are not precise enough (inaccuracy larger than  $5 \times 10^{-3}$  for the linear polarization degree or  $10^\circ$  for the linear polarization direction). The result is a unique determination of the average magnetic field vector of 296 quiescent

---

<sup>1</sup>Permanent Address: Observatoire Midi-Pyrénées, 14 Ave. E. Belin, F-31400 Toulouse, France

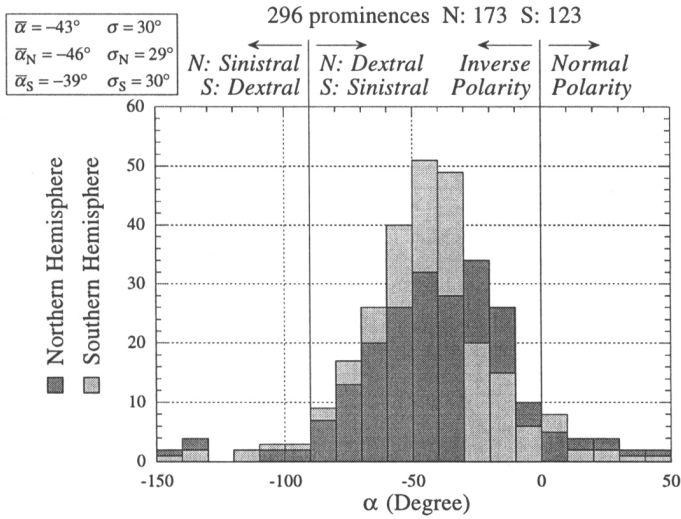


Figure 1. Histogram of the angle  $\alpha$  between the average field vector and the neutral line (following the definition of Leroy et al. 1984, Figure 4).

prominences corresponding to 2390 measurements.

## 2. Hanle Effect Interpretation

The full set of linear polarization data obtained with a single line (He I D3) has been reinvestigated by applying the results previously obtained from simultaneous observations of two lines of the same (He I D3 and H $\beta$ , 14 prominences, Bommier et al. 1986) and different (He I D3 and H $\alpha$ , 18 prominences, Bommier et al. 1994) optical thickness, namely the field vector close to the horizontal plane (dip of field line across the prominence) and inverse polarity with respect to the adjacent photospheric field. In the present analysis, the fundamental 180° ambiguity has been removed in a two-step procedure.

In the first step, the ambiguity has been removed in all cases where the two ambiguous solutions have opposite polarities, by selecting the inverse polarity solution (that we call the ‘polarity law’). This is the case for 264 of the full sample of 296 prominences. As the two ambiguous solutions are nearly symmetrical with respect to the line-of-sight, the method fails when the neutral line lies along a meridian because, in this case, the two ambiguous solutions have the same polarity. Most of these 264 prominences are found to obey the chirality law of Martin et al. (1994), already obtained at high latitudes by Leroy et al. (1983, see their Figure 5), i.e., dextral chirality in the northern hemisphere and sinistral chirality in the southern hemisphere.

In the second step the ambiguity has been removed for the 32 remaining prominences, using the above result that their two ambiguous solutions have the

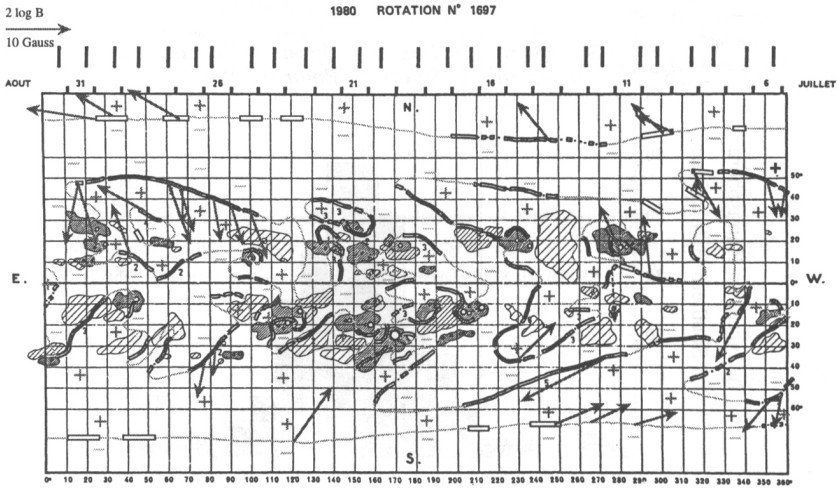


Figure 2. Rotation 1697. Each arrow has been scaled (in  $\log_{10} B$ ) to the average magnetic field vector of a prominence observed on a given day.

same polarity but opposite chiralities. (Because the two ambiguous solutions are nearly symmetrical with respect to the line-of-sight, this is strictly the case when the neutral line lies along a meridian). The solution selected for these prominences is the one having chirality in agreement with the chirality law.

As the two ambiguous solutions are nearly symmetrical with respect to the line-of-sight, the chirality-law method fails when the neutral line lies along a parallel of latitude, and the polarity-law method fails when the neutral line lies along a meridian. Where one of the two methods fails, the other method will apply. Thus, both methods are complementary and, in those cases where both methods apply, they give results in agreement for nearly all the cases. However, it must be emphasized that the chirality-law method is derived from the result of the polarity-law method. Also, by using this procedure, a few normal-polarity prominences are derived by using the chirality-law method and, accordingly, a few prominences are found to not obey the chirality law, using the polarity-law method to solve the ambiguity. Such 'exceptions' are preferentially found at places where the general direction of a neutral line is changing.

The results of the present analysis fully confirm previous ones (Leroy et al. 1983, 1984) in the limit of the measurement (and other causes of) inaccuracies. As an example, Figure 1 shows the histogram of the angle  $\alpha$  between the field vector and the neutral line, oriented as defined by Leroy et al. (1984, see Figure 4). Positive and negative  $\alpha$  angles correspond respectively to Normal and Inverse polarity. On the Figure, both hemispheres have been distinguished. In the northern hemisphere, the filament is dextral when  $\alpha$  lies inside the interval  $[-90^\circ, +90^\circ]$ , and sinistral outside (opposite for the southern hemisphere). The average value  $\bar{\alpha} = -43^\circ$  and standard deviation  $\sigma = 30^\circ$  do not contradict previous results  $\bar{\alpha} = -25^\circ$  and  $\sigma = 38^\circ$  (Leroy et al. 1984), due to the measurement

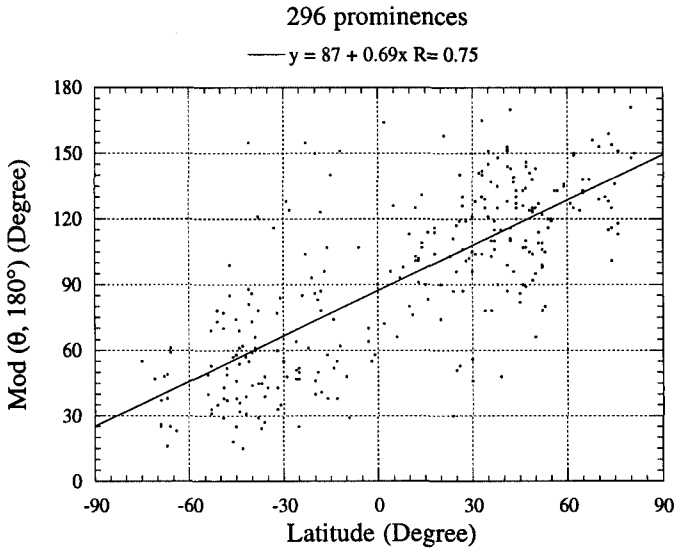


Figure 3. Angle  $\theta$  (modulo  $180^\circ$ ) between the average field vector of each prominence and the W-oriented solar parallel, as a function of the Latitude. Above, the equation and correlation coefficient of the linear least square fit.

(and other causes of) inaccuracies.

The results have been plotted on the synoptic maps of Meudon Observatory, along with data on the photospheric polarities and neutral lines taken from the McIntosh maps (NOAA/SEC). An example is given in Figure 2. Each arrow corresponds to the average magnetic field (in strength and direction) of a prominence observed on a given day. The full arrows (all except one on Figure 2) correspond to prominences for which the ambiguity has been removed by applying the polarity-law method. The dashed arrows (only one on Figure 2, at latitude  $7^\circ$  and longitude  $274^\circ$ ) correspond to prominences for which the ambiguity has been removed by applying the chirality-law method.

These maps show the evidence of a global pattern of the average magnetic field vector of prominences: global direction along a North-South line distorted by the differential rotation (see a linear least square fit in Figure 3), reversal of the field from a neutral line to the adjacent one in both E-W and N-S directions (a result previously obtained at high latitudes by Leroy et al. 1983), antisymmetry of the North and South hemispheres. Inverse polarity is found for both axial and transverse components of the magnetic field vector.

## References

- Bommier, V., Leroy, J.L., Sahal-Br  chot, S. 1986, *A&A*, 156, 79  
 Bommier, V., Landi Degl'Innocenti, E., Leroy, J.L., Sahal-Br  chot, S. 1994,

Solar Phys., 154, 231

Leroy, J.L., Bommier, V., Sahal-Bréchet, S. 1983, Solar Phys., 83, 135

Leroy, J.L., Bommier, V., Sahal-Bréchet, S. 1984, A&A, 131, 33

Martin, S.F, Bilimoria, R., and Tracadas, P.W. 1994, in Solar Surface Magnetism, (eds.) R. Rutten and C. Schrijvers, Kluwer Acad. Publ., Dordrecht, Holland, p. 303